Real-Time Eco-Driving for Connected Electric Vehicles

Caroline Ngo, Edwin Solano-Araque, Missie Aguado-Rojas, Antonio
Sciarretta, Bicheng Chen, Mohamed El Baghdadi

Real-time eco-driving
for connected electric vehicles

Caroline Ngo, * **Edwin Solano-Araque,** *
Missie Aguado-Rojas, * **Antonio Sciarretta,** * **Bicheng Chen,** **
Mohamed El Baghdadi ***

** IFP Energies Nouvelles, 1 et 4 avenue de Bois-Préau, 92852
Rueil-Malmaison Cedex, France (e-mail: caroline.ngo@ifpen.fr)
** RWTH Aachen University, Forckenbeckstr. 4, 52074 Aachen,
Germany (e-mail: chen$_b$@vka.rwth − aachen.de)
*** Vrije Universiteit Brussel, Pleinlaan 2, 1050 Brussel, Belgium
(e-mail: Mohamed.El.Baghdadi@vub.be)*

Abstract: This paper presents a real-time eco-driving algorithm for connected electric vehicles. The proposed solution generates a safe eco-speed profile, avoiding collision with the preceding vehicle and respecting the speed limits. An Eco-driving Optimal Control Problem (ED-OCP) is formulated minimizing the energy consumption of an electric vehicle while enforcing state (position, speed, acceleration) constraints. Analytical solutions of the state-constrained ED-OCP are implemented according to a model predictive control scheme. The proposed solution is evaluated using a connected simulation platform developed during the H2020 EU project CEVOLVER, under several driving scenarii, showing a significant energy consumption reduction.

Keywords: optimal control, eco-driving, connected electric vehicle

1. INTRODUCTION

Greenhouse emission reduction in transportation has become a priority, it represents the main cause of air pollution in cities. Emissions due to transportation represent 26% of the overall green house emissions in the European Union, of which road transportation represent 71% (European Environment Agency (2021)). The electrification of vehicles is considered as a promising way to reduce the pollutant emission in cities, or to suppress them in case of fully electrified vehicles. However, despite the many efforts from the manufacturers to increase the driving range of the electric vehicle (EV), range anxiety is still the main obstacle to its use.

Connectivity is a promising way to overcome this constraint. The connection to the cloud offers the possibility to predict and optimize energy consumption along a trip based on route topology information provided by a Geographic Information System (GIS), but also real-time information about the traffic, the weather, charging stations availability, among others. Moreover, connectivity between cars and infrastructure, namely V2X technologies, provides to each vehicle information about its surroundings, in order to anticipate the behavior of the neighboring vehicles and thus to act cooperatively to achieve safe and ecological driving.

Within this context, eco-driving aims to help the driver to adopt the most economic driving profile to reduce energy consumption. Many studies over the past decade have shown the interest of eco-driving as a direct mean to reduce the energy consumption of vehicles by acting on the driving style. One can distinguish between two main approaches to compute an eco speed profile. On the one hand, heuristic strategies which are based on eco-driving rules such as aggressiveness of the acceleration, stability of the cruising speed, anticipation and aggressiveness of the deceleration and braking, duration of idling, or optimal gear changing (Hof et al. (2012)). On the other hand, model-based strategies which use optimal control techniques to solve the eco-driving control problem.

The eco-driving problem can be formulated as an optimal control problem and solved in general using dynamic programming, direct methods (*e.g.* quadratic programming, interior point) or indirect methods. In Mensing et al. (2011), position constraint imposed by a preceding vehicle is introduced and dynamic programming is used to compute the constrained optimal solution that guarantees a minimum safety distance. Given its large computational burden, this solution cannot be implemented in real-time. In Paredes et al. (2019), the authors use a direct method to solve the eco-driving optimal problem in real-time for an electric bus between stops in dedicated lanes without safety considerations. More recently, solutions to computes an energy-efficient speed profile while guaranteeing safety constraints in speed and position showed results in simulation using analytical solutions (Han et al. (2019)), model-predictive control method (Wegener et al. (2020)) or reinforcement leaning (Wegener et al. (2021)).

The main challenge for an eco-driving algorithm dedicated to connected EVs is to provide in real-time a safe speed profile, anticipating the surrounding traffic disturbances to offer the maximum energy savings. The control should be robust to various driving scenarii. To that aim, this paper presents a real-time eco-driving algorithm for connected

EVs equipped with Advanced Driver-Assistance Systems (ADAS) or V2X technologies. The proposed approach is based on analytical solutions obtained by solving the optimal control problem with Pontryagin's Minimum Principle considering position and speed constrained situations. The optimal solution is applied following a model predictive control (MPC) scheme with a shrinking horizon. To ensure the control robustness, a feasibility analysis of the boundary condition is done.

The paper is organized as follows: in section 2 the Eco-Driving Optimal Control Problem (ED-OCP) is introduced. In section 3 the proposed approach and its real-time implementation are described. The connected simulation platform used for testing the proposed solution is presented in section 4. The results are shown and discussed in sections 5 and 6.

2. ECO-DRIVING CONTROL PROBLEM FORMULATION

The eco-driving strategy for EVs aims to propose to the driver an eco-speed profile $v^\star(t)$ that minimizes the battery electrochemical power consumption $P_{bat}(t)$ over the travel time horizon t_f, along a route segment of length s_f, under environmental constraints on the vehicle's position $s(t)$, speed $v(t)$, and acceleration $a(t)$ states.

In this paper, several environmental constraints are considered. To take into account surrounding traffic and safety, a position constraint is added with a minimum safe distance (δ_s) imposed by a leading vehicle at a position s_p, $s \leq s_p - \delta_s$. Also, infrastructure constraints are considered with the addition of a speed constraint, $v \leq v_{max}$ to respect the speed limit. A final speed v_f at the end of the route segment is imposed either by the leading vehicle or by the type of segment end (*i.e.* stop sign, traffic light, roundabout).

A general formulation of the ED-OCP is given by:

$$\underset{u(t)}{\text{minimize}} \quad J = \int_0^{t_f} P_{bat}\left(u_p\left(t\right), v\left(t\right)\right) dt \quad (1a)$$

$$\text{subject to} \quad \dot{s}\left(t\right) = v\left(t\right) \quad (1b)$$
$$\dot{v}\left(t\right) = f_v\left(v\left(t\right), s\left(t\right), u\left(t\right)\right) \quad (1c)$$
$$s\left(0\right) = s_i, \ s\left(t_f\right) = s_f \quad (1d)$$
$$v\left(0\right) = v_i, \ v\left(t_f\right) = v_f \quad (1e)$$
$$u_p^{min} \leq u_p\left(t\right) \leq u_p^{max} \quad (1f)$$
$$a_{min} \leq a\left(t\right) \leq a_{max} \quad (1g)$$
$$0 \leq v\left(t\right) \leq v_{max} \quad (1h)$$
$$s\left(t\right) \leq s_p\left(t\right) + \delta s \quad (1i)$$

Equations (1b) and (1c) refer to the system dynamics, (1d) and (1e) to the boundary conditions, and (1f), (1g), (1h), and (1i) to the control and states constraints. The control input u_p is the powertrain force F_p divided by the vehicle mass m.

The longitudinal dynamics of a vehicle of mass m is given by (1c) with

$$f_v = u_p(t) - \frac{1}{2m}\rho_a A_f c_d v^2 - g\left(c_r + sin\left(\alpha(s)\right)\right) - \frac{F_b}{m}$$

where ρ_a is the air density, c_d is the aerodynamic drag coefficient, A_f is the vehicle frontal area, c_r is the rolling resistance, $\alpha(s)$ is the road grade that depends on the vehicle's position s, and F_b is the brake force.

The battery electrochemical power P_{bat} is described by the approximated model

$$P_{bat}(t) = \eta_b^{-sign(u_p)} \left(k_0 + k_1 \frac{\gamma_m}{r_w} v(t) + k_2 \frac{\gamma_m^2}{r_w^2} v^2(t) \right.$$
$$+ k_3 m \eta_t^{-sign(u_p)} u_p(t) v(t)$$
$$\left. + k_4 \left(\eta_t^{-sign(u_p)} \frac{m r_w}{\gamma_m} \right)^2 u_p^2(t) \right) \quad (2)$$

where k_i, $i \in [0, 4]$, are tunable coefficients, γ_m is the drivetrain transmission ratio, r_w is the wheel radius, η_t is the driveline efficiency, and η_b is the battery-to-motor conversion efficiency.

3. ANALYTICAL SOLUTIONS APPROACH

To be adaptive to the surrounding disturbances, the eco-speed profile needs to be computed in real time with frequently updated measures. A model-based analytical solution approach suits a real-time implementation since it needs low computational burden compared to nonlinear programming solutions.

The analytical solutions are briefly introduced in this section. The reader should refer to Sciarretta and Vahidi (2020) for an in-depth discussion on the presented approach.

3.1 Analytical solutions

To derive analytical solutions of the ED-OCP using Pontryagin's Minimum Principle, several assumptions are made:

- no brake: $F_b = 0$
- no aerodynamic friction: $\rho_a A_f c_d = 0$
- constant slope: $\alpha(s) = \alpha_0$
- efficiencies $\eta_t = \eta_b = 1$
- in Eq. (2): $k_3 = 1$, $k_5 = k_6 = 0$
- input saturation is not explicitly considered: $u_p^{max} = -u_p^{min} = +\infty$

Although these assumptions might be strong, the corresponding ED-OCP solutions are implemented following a MPC scheme (see section 3.2), which iteratively compensates the deviations between the simplified model and the real system behaviour.

Under these assumptions (2) becomes:

$$P_{bat}(t) = m u_p(t) v(t) + b u_p^2(t)$$

where $b = k_4 m^2 r_w^2 \gamma_m^{-2}$.

Unconstrained solution   In the case where no position nor speed constraints are active, the solution to the ED-OCP is given by:

$$v^\star(t) = v_i + \left(\frac{6s_f}{t_f^2} - \frac{4v_i}{t_f} - \frac{2v_f}{t_f} \right) t - \left(\frac{6s_f}{t_f^3} - \frac{3v_i}{t_f^2} - \frac{3v_f}{t_f^2} \right) t^2 \quad (3)$$

Speed constrained solution When the speed is constrained by a maximum speed bound v_{max}, the optimal speed profile reads:

$$v^\star(t) = \begin{cases} v_i + \dfrac{2(v_{max} - v_f)}{t_1}t + \dfrac{v_{max} - v_i}{t_1{}^2}t^2 & \text{in } [0, t_1) \\ v_{max} & \text{in } [t_1, t_2] \\ v_f + \dfrac{2(v_{max}-v_f)}{t_f - t_2}(t_f - t) - \dfrac{v_{max}-v_f}{(t_f - t_2)^2} & \text{in } (t_2, t_f] \end{cases}$$
$$(4)$$

where t_1 and t_2 are the entry and exit times of the constrained arc and are defined as:

$$t_1 = \frac{3(v_{max}t_f - s_f)\sqrt{v_{max} - v_i}}{(v_{max} - v_f)^{\frac{3}{2}} + (v_{max} - v_i)^{\frac{3}{2}}}$$

$$t_2 = t_f - t_1\sqrt{\frac{v_{max} - v_f}{v_{max} - v_i}}$$

Position constrained solution The position of a leading vehicle during the optimization horizon t_f is predicted using its current position, speed, and acceleration as measured by an ADAS or a V2X system. These are denoted, respectively, $s_{p,0}$, $v_{p,0}$, and $a_{p,0}$. Under the assumption of constant acceleration, the predicted position $\tilde{s}_p$ and the predicted speed $\tilde{v}_p$ read:

$$\tilde{v}_p(t) = v_{p,0} + a_{p,0}t$$

$$\tilde{s}_p(t) = s_{p,0} + \int_0^t \tilde{v}_p(\tau)d\tau$$

The optimal speed profile considering the position constraint is given by:

$$v^\star(t) = \begin{cases} v_i + c_1 t + c_2 t^2 & \text{in } [0, t_c) \\ c_3 + c_4(t - t_c) - c_5\dfrac{(t - t_c)^2}{(t_f - t_c)^2} & \text{in } [t_c, t_f] \end{cases}$$
$$(5)$$

where t_c is the contact time that is found by solving the cubic equation:

$$(v_i - v_f + a_{p,0}t_f)t_c^3 + \left((4v_{p,0}+v_f-2v_i)t_f + \frac{a_{p,0}t_f^2}{2} - 3s_f\right)t_c^2$$
$$+ \left(6s_{p,0}t_f + (v_i - v_{p,0})t_f^2\right)t_c - 3s_{p,0}t_f^2 = 0$$

where the terms c_i are defined as

$$c_1 = a_{p,0} + \frac{4(v_{p,0} - v_i)}{t_c} + \frac{6s_{p,0}}{t_c^2}$$

$$c_2 = -\frac{6s_{p,0}}{t_c^3} - \frac{3(v_{p,0} - v_i)}{t_c^2}$$

$$c_3 = v_{p,0} + a_{p,0}t_c$$

$$c_4 = a_{p,0} - \frac{6s_{p,0}}{t_c^2} - \frac{2(v_{p,0} - v_i)}{t_c}$$

$$c_5 = v_f - 3v_{p,0} + 2v_i - 6\frac{s_{p,0}}{t_c} - a_{p,0}t_f + 6s_{p,0}\frac{t_f}{t_c^2}$$
$$+ 2(v_{p,0} - v_i)\frac{t_f}{t_c}$$

3.2 MPC approach

The analytical solutions of section 3.1 are implemented following a model predictive control scheme with a shrinking horizon approach.
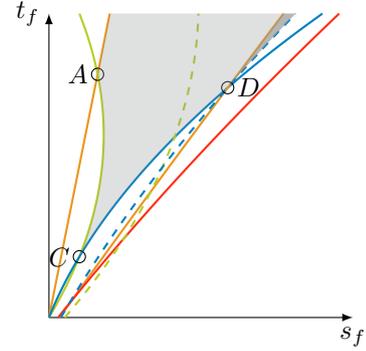

Fig. 1. Domain of feasibility: Light gray zone corresponds to the set of unconstrained solution, dark gray to the position constraint solution; the different curves correspond to the different feasibility conditions, tested to validate the $\{s_f, t_f\}$ and eventually correct them.

At every time step, one of the optimal solutions $v^\star$ given by (3), (4), and (5) is selected according to whether, at the current driving situations, a speed or position constraint is active or not. Then, the solution is computed until the end of the current horizon. As in model predictive control, only the first control is applied. This procedure is repeated using the updated measures at a time step of 100 ms to be adaptive to new situations.

The boundary conditions $\{v_f, s_f, t_f\}$ are derived from GIS information, in particular using the traffic average speed for the values of t_f and v_f. In case of the presence of a preceding vehicle, especially when the latter decelerates, the boundary conditions are adjusted to the preceding vehicle's trajectory prediction, obtained from $\{s_p(t), v_p(t), a_p(t)\}$. The values of $\{v_f, s_f, t_f\}$ are therefore time-varying and updated at each time step.

The analysis of these boundary conditions determines if the solution $v^\star$ is feasible. As an example, for given values of $v_i(t)$ and $v_f(t)$, the sets of feasible values of $\{s_f(t), t_f(t)\}$ can be computed as shown in figure 1. If the optimal solution is not feasible, the boundary conditions $t_f(t)$ or/and $s_f(t)$ are modified to fulfill the feasibility conditions. The minor adjustment tries to minimize the impact on the travel time. To guarantee the robustness of the control, an additional "preventive/emergency braking" mode is implemented, and is activated when the preceding vehicle brakes rapidly.

4. SIMULATION FRAMEWORK

The proposed algorithm is evaluated using the simulation platform shown in figure 2. This platform includes a surrounding environment model, a driver model which is sensitive to the environment influence, and a high-fidelity EV model. To simulate the eco-driving strategy, the platform is connected to a proprietary cloud from which it receives real-time and predictive data about the traffic, the weather conditions and the route. ADAS or V2X technologies such as radar or camera sensors are simulated.
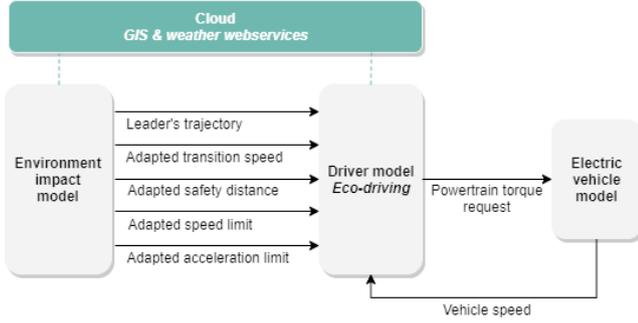
Fig. 2. Simulation platform

4.1 Driver model

The driver model is used in the simulation platform to follow the target speed profile generated by the eco-driving strategy or a car-following model, and provides powertrain torque demand to the EV model. Although in the simplified model of section 3.1 brakes are not considered, the driver model uses both the motor and the brake torques.

The eco-driving receives route information about a chosen trip. The eco-speed profile is computed along sub-trips defined either by the GIS or custom aggregation of short route's segments. The constraints on position, speed and acceleration are adapted according to the disturbances generated by the environment model along the route.

4.2 Environment model

The environment model simulates the impact of the surrounding vehicle's environment, namely the route and infrastructure, the traffic and the weather. The developed model acts on the driver model modifying the position, speed and acceleration constraints. The considered influences and their effect on the driver model are described in table 1.

Disturbance	Impacted variable on eco-driver
Leading vehicle	Position, speed
Route length	Speed profile
Route curvature	Maximum speed along the curvature for comfort and safety
Traffic signs	Transition speed at the end of segment
Legal speed limit	Cruising speed
Weather condition	Cruising speed, acceleration/deceleration, following distance to leading vehicle

Table 1. List of modeled influences

Route and infrastructure   The influence due to the route infrastructure is modeled thanks to third party mapping web-services. The eco-speed profile is enriched by taking into account the speed profile disruptions induced by the road signalization and infrastructure. Indeed, the GIS database contains information about the route topology, the legal speed limit and the type of interface ending each route segment (*e.g.* stop sign, traffic light, turning movement). To model the influence of the intersection on the driver's speed profile, the transition speed $v_{f,i}$ between two route segments $\{i-1, i\}$ is computed as:

$$v_{f,i} = \beta \frac{v_{avg,i} + v_{avg,i+1}}{2} \qquad (6)$$

where $v_{avg,i}$ and $v_{avg,i+1}$ are the average traffic speeds provided by the map web services, and $\beta \in [0,1]$ is a parameter depending on the type of interface, which could be selected in a deterministic or stochastic way. The driver model also adapts its speed profile to the route topology-induced constraints, in particular the vehicle speed limit due to route curvatures. The route curvature is reconstructed from the longitude and latitude coordinates along the chosen route to obtain the apparent route heading. From this heading and the vehicle-route static friction limit, the speed limit due to the curvature is obtained.

Surrounding traffic   A model of a leading vehicle is added to simulate the surrounding traffic. The idea relies on the fact that regardless of the overall traffic, the ego vehicle behavior mainly depends on the behavior of the immediately preceding vehicle. A virtual leading vehicle is modeled using Gipps' car following model [Gipps (1981)]. It follows the same planned route as the ego vehicle and is only sensitive to the route topology and infrastructure. The leading vehicle's speed profile is generated for each route segment, reproducing the behavior of a driver with no anticipatory abilities of the route to come.

Weather   A first impact of the weather condition is the adjustment of the legal speed limit. Indeed, in some countries the local legislation imposes to lower the legal speed limit in case of adverse weather conditions. A second impact is the influence in general of the weather condition on the driver behavior: the latter will adapt the safety distance and acceleration (or deceleration) concerning, for instance, the visibility in a rainy situation or the drift risks in cold conditions. To anticipate the influence of the weather condition, the state constraints of the ED-OCP are adapted, modifying the maximum acceleration/deceleration and the minimum distance gap, as described in Hammit et al. (2018).

5. SIMULATION RESULTS

The performance of the eco-driving algorithm is evaluated using two urban trips of 4.2 km and 5.3 km, shown in figure 3. The selected trips are located in congested areas in order to assess the impact of traffic constraints on the speed profile, and thus bring out the performance of the presented connected eco-driving algorithm.
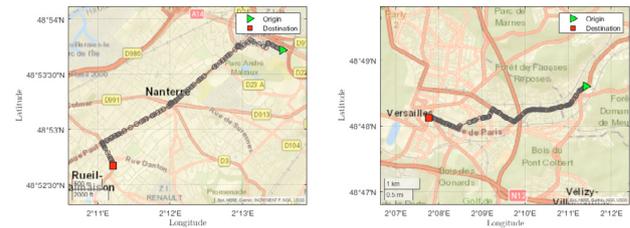

Fig. 3. Validation urban trips 1 (left) and 2 (right) (*circles indicate nodes*)

For the two tests, a vehicle (Leader) is always in front of the controlled vehicle (Ego) in order to simulate the surrounding traffic as described in the previous section (see fig. 4). To evaluate how the proposed approach adapts

to the vehicle's surrounding disturbances and the gain obtained with the eco-speed profile, a comparison is done with respect to a speed profile generated by the Gipps car-following model so as to represent a non-eco-driving vehicle. Both vehicles drive on the same route with the same travel time to have a fair comparison. The constraint v_{max} of the Gipps model is set to a value between the legal speed limit and the traffic average speed to obtain the same travel time. Therefore, the ego Gipps average speed is lower than the leading vehicle one.
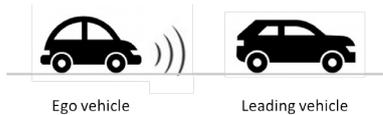
Fig. 4. Surrounding traffic simulation : Leading vehicle (Gipps) always in front of Ego vehicle (Gipps or eco-MPC)

The eco-driving adapts its trajectory to avoid unnecessary acceleration/deceleration between route segments thanks to the route information and provides a smooth speed profile while preventing collision with the leading vehicle. One can observe in figure 5 that the solution respects the safety distance imposed by the leading vehicle along the trip.
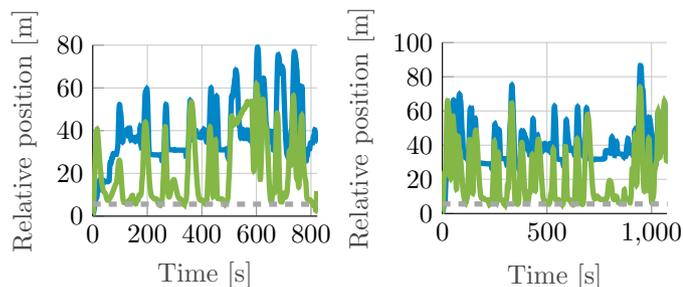

Fig. 5. Relative position to the leading vehicle in Trip 1 (left) and 2 (right) (*blue: Gipps, green: eco-MPC, dotted: δ_s*)

The Gipps driver model does not know the route to come, hence sharp accelerations and decelerations can be observed at the beginning and the end of each route segment despite the fact that the ego vehicle stands relatively far away from the leading vehicle. The acceleration distributions (figs. 6 and 7) reflect those behaviors: the eco-MPC has a centered acceleration distribution with few observations at its ends, whereas the Gipps model's distribution tends to have bigger left and right tails, showing that greater deceleration and acceleration values occur more frequently.

The eco-driving obviously impacts the speed. In figure 8, cumulative distributions of the speed for the two trips show that the target speed generated by the eco-MPC is lower than the speed of the reference Gipps model. As a consequence, the energy consumption of the non-eco-driving vehicle tends to increase.

The figure 9 shows a focus on the speed profile at the beginning of the trip between 0 and 1.2 km and the
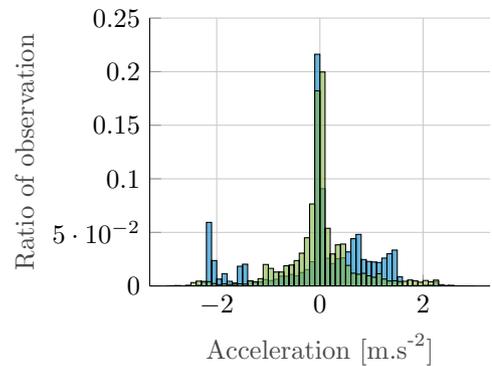

Fig. 6. Vehicles' accelerations distribution in Trip 1 (*blue: Gipps, green: eco-MPC*)
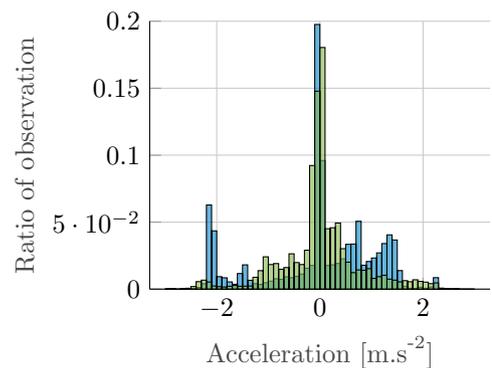

Fig. 7. Vehicles' accelerations distribution in Trip 2 (*blue: Gipps, green: eco-MPC*)
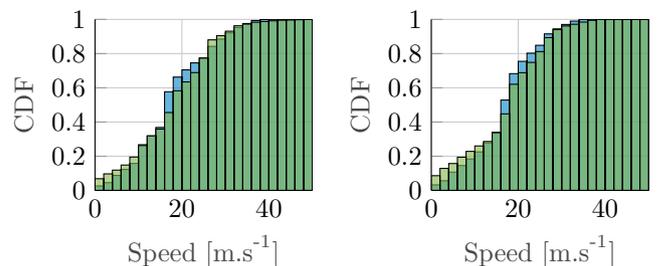

Fig. 8. Vehicles speed cumulative distribution in Trip 1 (left) and 2 (right) (*blue: Gipps, green: eco-MPC, dotted: δ_s*)

impact of the Gipps behavior on the energy consumption which increases faster than the eco-MPC one, in particular between 200 m and 500 m.
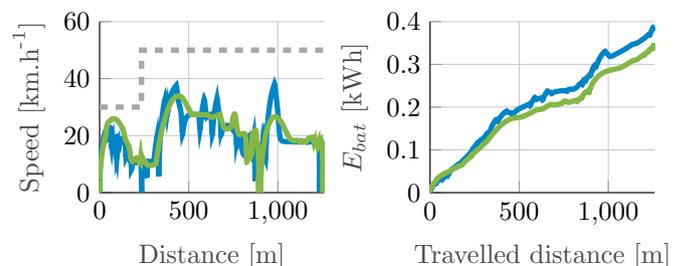

Fig. 9. Vehicles speed profiles (left) and energy consumption (right)

A focus on the partition of the energy consumption for the two trips are given in figures 10 and 11. The calculations of the different non-reducible energy components, namely the variations of kinetic, potential, rolling resistance and auxiliaries energies, is detailed in Sciarretta and Vahidi (2020). For equivalent scenarios, the effective energy consumption, denoted "other", is the only term impacted by the driving behavior. The results show that the battery energy consumption has been reduced by 9.2% for trip 1 and 13% for trip 2, corresponding to a reduction of 22.5% and 23%, respectively, for the effective energy.
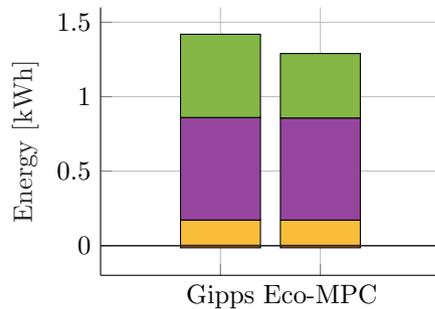

Fig. 10. Energy consumption results in Trip 1 (*blue: kinetic, red: potential, yellow: rolling resistance, purple: auxiliaries, green: others*)
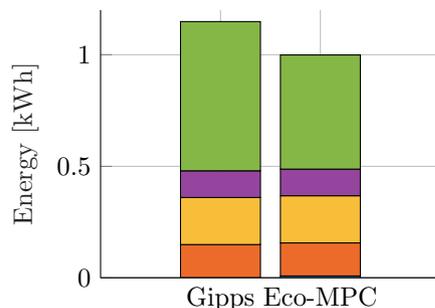

Fig. 11. Energy consumption results in Trip 2 (*blue: kinetic, red: potential, yellow: rolling resistance, purple: auxiliaries, green: others*)

6. CONCLUSION

This paper has presented an analytical approach to solve the ED-OCP under speed and position constraints for connected EVs. Implemented as a shrinking horizon MPC, ED-OCP is solved in real-time guarantying the generation of a safe eco-speed profile. The simulation platform used to test the proposed solution includes an environment model to emulate the surrounding impacts due to traffic, infrastructure and weather on the controlled vehicle. Promising results have been obtained within this platform. The analysis shows that in an urban situation the eco-MPC reduces the number and smooths the acceleration/deceleration while keeping as much as possible a constant speed to gain energy consumption. This strategy is consistent with the results reported in Solano Araque et al. (2018).

Future work will evaluate the sub-optimality of the presented solution with a reference optimal solution obtained

with a nonlinear optimisation approach. A better consideration of the leading vehicle's trajectory will be done to improve the anticipatory capability of the approach and further smooth the eco-speed profile. Finally, this algorithm will be embedded in EV and tested on open road within the framework of the project CEVOLVER.

ACKNOWLEDGEMENTS

REFERENCES

European Environment Agency (2021). Greenhouse gas emissions from transport in Europe.

Gipps, P. (1981). A behavioural car-following model for computer simulation. *Transportation Research Part B: Methodological*, 15(2), 105–111.

Hammit, B.E., Ghasemzadeh, A., James, R.M., Ahmed, M.M., and Young, R.K. (2018). Evaluation of weather-related freeway car-following behavior using the shrp2 naturalistic driving study database. *Transportation Research Part F: Traffic Psychology and Behaviour*, 59, 244–259.

Han, J., Vahidi, A., and Sciarretta, A. (2019). Fundamentals of energy efficient driving for combustion engine and electric vehicles: An optimal control perspective. *Automatica*, 103, 558–572.

Hof, T., Conde, L., Garcia, E., Iviglia, A., Jamson, S., Jopson, A., Lai, F., Merat, N., Nyberg, J., Rios, S., et al. (2012). A state of the art review and user's expectations. *European Comission ecoDriver Project*.

Mensing, F., Trigui, R., and Bideaux, E. (2011). Vehicle trajectory optimization for application in eco-driving. In *2011 IEEE Vehicle Power and Propulsion Conference*, 1–6.

Paredes, J.F., Cazar, G.P., and Donkers, M. (2019). A shrinking horizon approach to eco-driving for electric city buses: Implementation and experimental results. *IFAC-PapersOnLine*, 52(5), 556–561. 9th IFAC Symposium on Advances in Automotive Control AAC 2019.

Sciarretta, A. and Vahidi, A. (2020). *Energy-Efficient Driving of Road Vehicles - Toward Cooperative, Connected, and Automated Mobility*. Springer, Switzerland.

Solano Araque, E., Colin, G., Cloarec, G.M., Ketfi-Cherif, A., and Chamaillard, Y. (2018). Energy analysis of eco-driving maneuvers on electric vehicles. *IFAC-PapersOnLine*, 51(31), 195–200. 5th IFAC Conference on Engine and Powertrain Control, Simulation and Modeling E-COSM 2018.

Wegener, M., Koch, L., Eisenbarth, M., and Andert, J. (2021). Automated eco-driving in urban scenarios using deep reinforcement learning. *Transportation Research Part C: Emerging Technologies*, 126, 102967.

Wegener, M., Plum, T., Eisenbarth, M., and Andert, J. (2020). Energy saving potentials of modern powertrains utilizing predictive driving algorithms in different traffic scenarios. *Proceedings of the Institution of Mechanical Engineers, Part D: Journal of Automobile Engineering*, 234(4), 992–1005.